Deconvolution models for determining the real surface composition of InP (100) after bombardment with 5 keV Ar ions at different angles

R.Q. Odendaal and Johan B. Malherbe
Department of Physics, University of Pretoria, 0028 Pretoria, South Africa

pacs{82.80.Pv, 79.20.Rf, 79.20.Ap, 61.72.Vv}

Highlights

• New method to determine bombardment-induced surface composition changes.
• Angle-resolved Auger electron spectroscopy with a CMA.
• Deconvolution of depth profiles.
• Preferential sputter occurs in Ar-bombarded InP.

Abstract

Low energy ion bombardment can induce compositional changes in the surfaces of compound materials. A fundamental problem is to determine which of the two main mechanisms caused the compositional change, viz. preferential sputtering or bombardment-induced segregation. This paper describes a method, using Auger electron spectroscopy (AES) taken at different angles, to determine the real (top) surface concentrations for an InP (100) surface after 5 keV Ar^+ bombardment at varying impact angles. This bombardment results in an altered near-surface layer. This altered surface layer is amorphised and has a non-stoichiometric surface composition. AES intensity measures the average concentration over the information depth. In this paper, two deconvolution models were used to determine concentration vs depth distributions from the AES intensities. These two models were then used to calculate a surface concentration for each case. Using a deconvolution model in which chemical effects and segregation dominate, the calculated surface concentration was larger than 1, indicating an unphysical surface concentration. Applying a ballistic deconvolution model in the quantification equation, the surface concentration values determined, agree within 5% to the values obtained from TRIDYN simulations. From this follows that argon ion bombardment-induced compositional changes in InP are mainly due to preferential sputtering and ion beam mixing and (to a lesser extent) bombardment-induced diffusion.

Keywords: InP, Auger electron spectroscopy, ion bombardment, surface composition, deconvolution

1. Introduction

Low energy (100 eV – 20 keV) ion bombardment of solids has several applications in industry and in research. There are several different sputter deposition systems to make different types of coatings on substrates for a variety of applications. The drive to smaller devices has led the electronics industry to use low energy ion implantation to dope the semiconductor substrates [1]. Device characterisation is routinely used during prototyping and production. Of the characterisation techniques, surface analysis is used to study, for example, the effect of cleaning procedures on the surface composition and morphology. In many of the techniques, ion beams are used as the probing/analyzing tool, e.g. SIMS, ISS, etc. In other techniques, argon ion bombardment is ubiquitously used to sputter clean the surfaces or to sputter etch the samples to perform depth profiling [2].

Ion bombardment of compound substrates may lead to compositional changes in bombardment-induced modified region. For most of the abovementioned applications and for many other ion beam applications, such compositional changes can have negative consequences. Consequently, understanding the mechanism(s) leading to these changes can help design bombardment conditions or analysis methods minimizing this deleterious effect. A particular example illustrating this point is in quantitative Auger electron spectroscopy (AES) or X-ray photoelectron spectroscopy (XPS) using matrix correction factors [3]. In this methodology a sputter correction factor can be introduced to correct the bombardment-induced surface compositional changes [4].

Although there are slightly different definitions (see e.g. [5]) the term preferential sputtering is used when the mechanism for such compositional changes arise from ballistic collisions between the bombarding ion and the substrate atoms [6-9]. However, ion bombardment can result in substantial thermodynamic processes which can also lead to compositional changes. These radiation enhanced diffusion (RED), radiation-induced (Gibbsian) segregation (RIS), as well as recoil mixing phenomena, can be interrelated and complementary with the ballistic effects [7]. In line with the above argumentation, this paper describes a method by which it is possible to determine which mechanism is causing bombardment-induced surface compositional changes in a particular substrate using AES (or XPS) measurements taken at different angles, i.e. angle resolved AES (XPS).

It is generally accepted that the two main mechanisms that cause bombardment-induced compositional changes in semiconductor surfaces are preferential sputtering and radiation-induced segregation. Several studies have shown that the noble gas ion bombardment-induced compositional changes in GaAs are primarily due to radiation-induced segregation [10 - 13]. On the other hand, for InP it has been speculated that preferential sputtering, primarily dependent on the large mass

difference between the In and P components, is the dominant mechanism operating during ion bombardment that leads to a modified surface layer [12, 14-19]. However, there have been a few studies [20–22] suggesting that radiation-induced segregation plays an important role in the bombardment surface compositional changes in InP.

To ascertain which mechanism (preferential sputtering or radiation-induced segregation) dominates in a particular substrate species, extensive measurements are needed of samples bombarded at a whole range of temperatures. In the absence of such temperature measurements, the distributions of the substrate atomic species below the bombarded surface need to be determined. Usually, segregation effects cause an enrichment of a certain atomic species on the top surface with a depletion of the same species below the first monolayer and extending over several monolayers and a gradual increase of that species at greater depths to that of the bulk value – for a schematic profile see [23]. The sputter ejection of substrate atoms occurs predominantly from the top-most layer [24]. For this reason preferential sputtering will cause an exponential decay depth profile, ending in the bulk value, of the species with the lowest preferential sputter yield. Apart from sputtering, the incident ions also cause ion beam mixing of the substrate atoms over the range of the ion path as well as the creation of point defects such as vacancies and interstitials in the substrate. The latter can lead to enhanced diffusion of some of the substrate species. Therefore, a dominant preferential sputtering mechanism does not exclude an atomic depth profile extending deeper than the range of the bombarding ions. From the above discussion it follows that for room temperature ion bombardment, the depth distribution of the different atom species near the surface may indicate which mechanism(s) is/are operating during noble gas ion bombardment.

Compositional changes in InP surfaces, due to argon bombardment, have been studied extensively (e.g. see references in [7]. In this study the changes in the instantaneous surface composition of InP measured with Auger electron spectroscopy (AES) after bombardment with argon ions at different angles of incidence are presented. It is, however, known that the analysis depth of AES extends over several monolayers resulting in an average composition. This makes comparison with other analysis techniques with different analysis depths extremely difficult. Furthermore, the analysis depth of AES strongly depends on the geometrical setup, i.e. the orientation of the sample with respect to the analyser and the excitation electron beam. In different Auger systems, different average compositions will therefore be measured, again complicating comparisons between measurements. The negative aspects, such as varying analysis depths when varying the orientation of the sample with respect to the incident ion beam (and subsequently also with respect to the analyser) can be turned into positive use by applying principles analogous to angle resolved XPS (X-ray photoelectron spectroscopy). By deconvoluting the AES signal, the different sampling depths can yield information on the distributions of the different substrate atomic species as a function of depth below the (sputtered) surface. This is done in the current paper by taking two scenarios into account. Firstly a mechanism where

chemical effects like radiation-induced and/or Gibbsian segregation and diffusion, are dominant. Secondly, we consider a mainly ballistic mechanism (i.e. preferential sputtering and atomic mixing with some atomic diffusion) being the cause of atom redistribution in the near-surface layer of the target.

2. Experimental

An InP (100) S-doped wafer was cleaved to provide analytical samples. The samples were degreased by rinsing in trichloroethylene. The samples were then clamped to stainless-steel sample holders, with angles of between 20° and 90° with respect to the horizontal axis of the vacuum chamber, and the cylindrical mirror analyser (CMA) axis.

The InP samples were sputtered with argon ions of 5~keV energy, using a Physical Electronics Model 04-191 ion gun, mounted on the vacuum chamber at 19° to the vertical axis of the vacuum chamber. The experimental setup has been shown in previous papers [14], [18], [25]. The ion beam current was 2 to 2.5 μA, giving a current density of approximately 0.2 A cm^{-2}. The electron beam was mounted coaxially with the CMA axis, which is horizontal with respect to the sample. The base pressure of operation was less than 2×10^{-9} Torr, while the chamber was backfilled to a pressure of 5×10^{-5} Torr with the argon gas during ion sputtering. The ion beam current was measured using a Faraday-cup, and the energy of the ion beam was 5 keV. The samples were sputtered with a suitably high fluence (5×10^{16} Ar^{+} cm^{-2}) to ensure steady-state sputtering.

After reaching the steady-state, AES measurements were made using a Physical Electronics 545 Auger spectrometer equipped with a Model~110A cylindrical mirror analyser (CMA). The phosphorus $L_{III}M_{23}M_{23}$ (123 eV) and indium $M_{V}N_{45}N_{45}$ (405 eV) Auger peak intensities were digitally recorded using a PC137 interface. The intensity ratio I_{In} / I_{P} was measured from the differentiated spectra which were obtained using a 5 point Savitzky-Golay differential filter [26].

Quantification of the sputtered surface compositions needs an internal standard surface, i.e. the intensity ratio of unsputtered phosphorus and indium peaks I_{In}^{0} / I_{P}^{0}. To produce such a standard surface, some InP samples were cleaved *in vacuo* to produce InP(110) surfaces. The InP(110) surface was assumed to provide stoichiometric InP with very nearly the same matrix as that of the sputtered surfaces.

The results for the (non-deconvoluted) intensity ratio I_{In} / I_{P} at the different angles were very similar as those reported in [18], which were obtained using basically the same Auger electron spectrometer but with a lock-in amplifier. The latter gave directly the differentiated spectrum.

3. AES measurements

The quantitative composition within the analysis depth was determined by comparing the Auger peak signals with those from the stoichiometric (110) InP surface. These measurements were obtained after steady state sputtering at a fluence of 5×10^{16} ions.cm^{-2}, with an argon ion energy of 5 keV. The same steady state ratio of In to P Auger peaks was already obtained at much lower fluence, i.e. typically after an fluence of 1×10^{15} ions.cm^{-2}.

The majority of the sputtering and AES measurements were done on the (100) surface. However, measurements were also performed on vacuum-cleaved (110) surfaces. These surfaces were primarily used for the quantification (acting as a standard surface, i.e. a surface with known composition and with a similar matrix). The AES measurements on the (110) surfaces after sputtering gave within experimental error the same sputtered surface composition as similar measurements on the (100) surfaces; this is due to the amorphisation of the near-surface of the InP crystal.

All the samples developed surface roughness or topography because of the ion bombardment. The extent of the roughness depended on the ion fluence [27], the angle of incidence of the ions [28], ion energy [29] and ion species. Although the roughness increased with fluence, no fluence effect on the resulting surface composition was observed in this study for fluences between $5 \times 10^{15} \leq \phi \leq 1 \times 10^{17}$ ions.cm^{-2}. The topography development was maximized for angles of incidence near 40°. A comparison with the angular dependence of the surface composition and the fluence dependence indicates that topography development (albeit severe) did not play any role in the equilibrium sputtered composition. A similar observation was also reported in [18].

4. Analysis of the AES measurements

4.1 Depth deconvolution of AES measurements

Owing to the geometry used in the experimental setup, the measured Auger intensities at each different angle of incidence of the ions was also at a different angle of electron incidence and effective acceptance angle of detection in the CMA. Hence, the analysis depth will differ for each angle - a major disadvantage for a direct comparison of the measured intensities. The measured intensities can be deconvoluted to provide us with an estimate of the real surface concentration, by correcting for the difference in sampling depth. The effective attenuation length of Auger electrons λ for each element i is given by

$$\lambda_i = \lambda_i^0 \cos \varphi \qquad (1)$$

where the attenuation length λ_i^0 at normal incidence is corrected for elastic scattering shortening of the Auger electron [30], and φ is the angle of emission of the detected Auger electron with respect to the sample normal. For a CMA, a mean cosine of the angle of emission can be defined [31], depending on the sample-analyser axis geometry. The measured Auger intensity of component *i* is then given by

$$I_i = \frac{I_i^0}{\lambda_i} \int_0^\infty r_i(z) \cdot C_i(z) \exp\left(-\frac{z}{\lambda_i}\right) dz \qquad (2)$$

where $r_i(z) \geq 1$ is the backscattering factor, taken to be constant in depth but dependent on emission angle, and $C_i(z)$ is the mole fraction concentration at a depth z. The backscattering factors for the different angles of incidence of the electron beam were calculated using Shimizu's equations for 0°, 30°, and 45° [32]. The values at these three angles are used and assuming that $r_i = 1$ at a 90° angle of incidence [33] a fourth-order polynomial fit was made for In and P, from which the backscattering factors for all other angles of incidence were calculated. The inelastic mean free paths in the equation (2) was determined using the TPP-2M method [34] as $\lambda_{In} = 1.28$ nm and $\lambda_P = 0.62$ nm..

During ion sputtering, compositional changes take place to a depth proportional to the ion range. The behaviour of the concentration profile, $C_i(z)$, is thus somewhat unsure, but based on analyses done with other techniques, such as angle-resolved XPS [11] certain estimates can be made for the general shape of the profile $C_i(z)$. Different sputter mechanisms can be tested by choosing a corresponding profile $C_i(z)$ and then deconvolute the data with this choice of $C_i(z)$. In the next two subsections, the deconvolution will be discussed using models based on different atomic redistribution mechanisms; firstly, a mechanism where chemical driving forces dominates, and secondly a ballistic mechanism.

The composition depth profile $C_i(z)$ was also estimated by the ion bombardment simulation code TRIDYN [35]. A full description of this is given in section 4.4.. In addition to this simulation, the projected ranges of the implanted ions were calculated using the Monte Carlo programme SRIM [36].

4.2 Chemical driving forces: Segregation and diffusion induced redistribution

The sputtering of target surfaces is a highly complex dynamical process during which the different target species as well as the ion are mixed due to the collision cascade. This mixing is the result of many interplaying processes. During ion sputtering, vacancies are formed which can induce a diffusion gradient. Segregation of inner target atoms can also be enhanced by such a vacancy connected transport mechanism. Simple atom erosion from the surface or near-surface is a further method of creating

an altered surface layer.

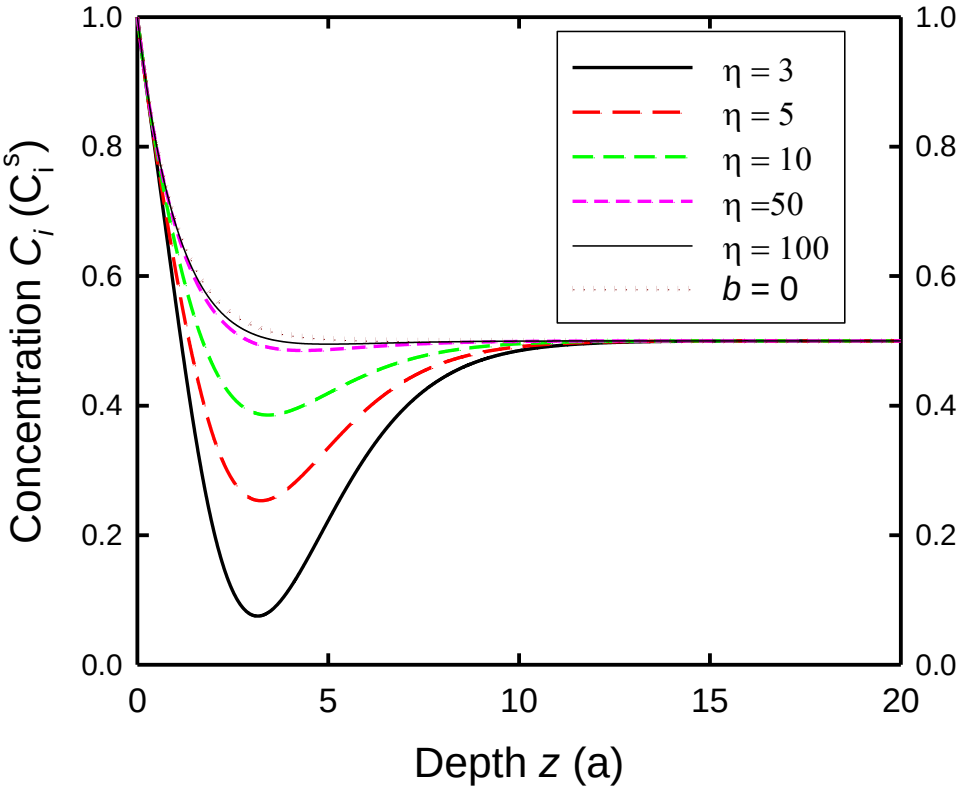

Figure 1. Molar fraction concentration profiles $C_i(z)$ of species i, in units of the instantaneous surface mole fraction C_i^s, obtained from equation (3) for different values of the dimensionless parameter $\eta = 1/(ba^3)$. For large values of η, i.e. b ≈ 0, the purely ballistic profile described by equation (5) is also shown. The bulk concentration of a binary compound is $C_{b\_} = C_i(\infty) = 0.5$ The unit for the depth scale is the parameter a in equations (3) and (5).

As was discussed in the Introduction, in sputtering the substrate atoms are predominantly ejected from the top-most layer [24]. Thus in both preferential sputtering and radiation-induced segregation the depth profiles of the individual species will have some measure of an exponential behavior. In the case of pure preferential sputtering the non-preferentially sputtered species will exhibit an exponential decay depth profile; or one which will be very nearly exponential. Such a profile is shown by the curve $b = 0$ in Figure 1. For radiation-induced segregation there is an enrichment of a certain atomic species on the top surface with a depletion of the same species below the first monolayer and extending over several monolayers and a gradual increase of the species, at great depths, to that of the bulk value. A typical profile of the segregating species (see also [23]) is the curve η = 3 in Figure 1. In order to have an analytical expression to describe these two bombardment-induced compositional changes we propose to use

$$C_i(z) = \frac{1}{2} + \left(-bz^3 + C_i^s - \frac{1}{2} \right) \exp\left(-\frac{z}{a} \right) \qquad (3)$$

where $C_i(z)$ is the molar fraction concentration of component i, $C_i^s = C_i(0)$ is the instantaneous surface mole fraction, a is a parameter associated with the thickness of the resultant modified layer due to ion sputtering, b determines the dip in the segregation profile, i.e. the dominance of radiation-induced segregation. The factor ½ comes from the fact that we consider a binary compound. The unit of the depth scale is a, which appears in the exponential term in (3).

It is reasonable to expect that in some binary systems both preferential sputtering and radiation-induced segregation can occur simultaneously. In order to describe such a system, the dimensionless parameter $\eta = 1/(ba^3)$ is a useful one. As can be seen from Figure 1, bombardment-induced compositional profiles where radiation-induced segregation effects dominate are describe best by smaller values of η, while for very large values of η, the profiles approach the profile $b = 0$, i.e. pure preferential sputtering. The latter case is also described by equation (5), which is given and discussed in section 4.3. In the case of only bombardment-induced segregation, i.e. no preferential sputtering of one of the species, there is no loss of atomic species in this case. Therefore, the areas below and above the bulk concentration level (representing a stoichiometric concentration) should then be equal. We shall use this fact later to give a value for η when this occurs.

The profiles given by equation (3) are very similar to the ones obtained from argon bombarded GaAs with Laplace transformations of the ARXPS signals by Bussing *et al*. [11] and by Valeri *et al*. [12] using sputter depth profiling AES. Bussing *et al.* [11] identified radiation-induced segregation to occur in the sputtering of GaAs. On the other hand, the depth profiles of sputtered InP by Valeri *et al*. [12] correspond to the $b = 0$ case above.

The profile of the implanted ions is very near to a Gaussian distribution with a projected range R_P and projected range straggling ΔR_P. Because low energy ions were used in this study, one can expect $R_P \approx \Delta R_P$ and that the damaged or altered layer will also be Gaussian with approximately the same values for the profile parameter, i.e. the projected range of damage $R_{d\_} \approx R_P$ and $\Delta R_{d\_} \approx \Delta R_P$. From Figure 1 it can be seen that for a depth of around 15a units, a constant concentration has been reached, *viz.* the bulk concentration. Consequently one would expect that
$15a \approx R_P + 2\Delta R_P \approx 3R_P$. The projected ranges R_P for 5~keV argon ions in InP for the different angles of incidence employed, were calculated using the SRIM code [36] and these values were subsequently used to calculate the values of the parameter a.

As was argued above, in the case of only bombardment-induced segregation taking place, the areas below and above the bulk concentration level should be equal. This means that

$$\int_0^{\infty}\left[C_i(z)-\frac{1}{2}\right]dx=\int_0^{\infty}\left[\left(-bz^3+C_i^s-\frac{1}{2}\right)\exp\left(-\frac{z}{a}\right)\right]dx=0 \qquad (4)$$

In terms of the units of $C_i(z)$, i.e. C_i^s, this integral leads to $b = 1/(12a^3)$. Deconvoluting the AES data with equation (2) for this particular value for b gave a value for $C_i^s > 1$. This is physically not possible because according to our definition of the concentration in mole fractions, $0 \le C_i^s \le 1$. This indicates that it is highly unlikely that the change in the Auger In to P peak ratios after ion bombardment is caused by stoichiometric sputtering of InP (i.e. non-preferential sputter) and only bombardment-induced segregation.

Deconvoluting the AES data with equation (2) for general values for b shows that concentration profiles for which $0 \le C_i^s \le 1$, can only be obtained for $3 \le \eta \le 12$. If, however, the additional constraint of $a = R_P/5$ is brought in, then such solutions could only be obtained for $\eta \approx 10^5$. This high value for η makes b << 1; thus making the influence of segregation very small. This means that the exponential term (the preferential sputtering and mixing term) dominates. This again indicates that it is highly unlikely that bombardment-induced segregation plays a major role in bombardment-induced compositional changes in InP.

4.3 Ballistic redistribution: Preferential sputtering and atomic mixing

The analysis given in the previous subsection has already clearly shown that preferential sputtering, together with a mixing process, is the major bombardment-induced compositional change mechanism in InP. However, the equation (3) used, is unnecessary complicated. A ballistic mechanism can be modelled by a far more simple, two parameter equation.

For the preferential sputtering case, it means that most of the material removed comes from the outer atomic layers. Mixing of the target atoms occurs throughout the altered layer, up to a depth more or less equal to the projected range of the bombarding ions.

Before the steady-state is reached, the concentration profile is dynamic. Steady-state is reached when the sputtered particles is in the same ratio as the bulk concentration of the components. It is reasonable to assume that due to the continuous sputtering of the surface material, the composition profile inside the material due to ion beam mixing will, under steady-state conditions, have an exponential behavior. As was discussed previously, the depth profile when only preferential sputtering occurs, is also exponential. Consequently, we propose that the profile to model a purely ballistic induced mechanism (see Figure 1) is given by

$$C_i(z)=\frac{1}{2}+\left(C_i^s-\frac{1}{2}\right)\exp\left(-\frac{z}{a}\right) \qquad (5)$$

where C_i^s is the surface mole fraction of component i, and a is a parameter associated with the thickness of the resultant modified layer due to ion sputtering. If the value $b = 0$ is substituted into equation (3) it becomes equal to (5). This model clearly does not include a term to make provision for any ion implantation. It is thus assumed in this deconvolution model that ion implantation does not influence the sputter yield in a major way even though there have been reports of argon ion implantation lowering the sputter yield of SiC [37]. Although the compositions as calculated by TRIDYN include the implanted Ar due to the sputtering by Ar ions, we renormalized the concentrations as calculated by TRIDYN to ignore the Ar fractional composition. This was done in order to agree with our model concentration given by equations (3) (and (5)).

From Figure 1 it can be seen that the concentration given by curve $b = 0$ becomes approximately equal to the bulk concentration (i.e. ½) at a depth $z = 6a$. Thus, we estimated that the altered layer thickness produced by the ballistic model (i.e. for $b << 1$) is of the order of $6a$.

Estimating the value of a is not clear cut; SRIM was used to calculate the projected ranges for 5 keV argon ions in InP for different angles of incidence and are given in Table 1.

Table 1. Ion angle of incidence θ_j dependence of the projected range R_P as calculated using SRIM 2000.38 [36]. The a parameter as estimated from a TRIDYN simulation depth profile fit of equation (5) for 5keV Ar^+ ions in InP is also shown.

Angle of incidence θ_j	**Project range R_P (nm) SRIM2000.38**	***a* as fitted from TRIDYN (nm)**
1°	8.1	8.4
11°	8.1	8.3
21°	7.8	7.6
31°	7.3	7.5
41°	6.9	6.4
51°	6.2	5.2
61°	5.7	4.6
71°	5.2	3.5

The shape of the curve of equation (5) is very similar to that found by Valeri *et al.* [12] for argon ion bombardment of InP. Zemek *et al*. [22] also determined similar depth profiles for the atomic species for argon ion bombarded InP, but at the very low temperature of 150 K. At this low temperature, diffusional and segregational

movement by substrate atoms will be minimal, leaving only purely ballistic redistribution for any compositional change.

4.4 TRIDYN simulations

To make a better estimate of the *a* parameter, the TRIDYN [35] package was used to calculate the depth distribution of target atoms in InP after being subjected to 5 keV Ar^+ ions at a fluence of 5×10^{16} Ar^+ cm^{-2}. The TRIDYN simulations ignore the effect of argon ion implantation, as already mentioned, by re-emitting all ions from the crystal. It, furthermore, does not simulate long range diffusion of the substrate atomic species. The simulations were done using 10^6 particle histories. The surface (actually the surface and near-surface) concentration was averaged by TRIDYN over a thickness of 1 nm from the dynamical depth distribution. The other relevant simulation parameters are given in Table 2. The simulations were repeated for various angles of ion incidence, i.e. $\theta_j = 1°, 11°, \ldots 71°$.

Table 2. TRIDYN simulation parameters. The sublimation energy [38] was used for the surface binding energy E_s; the displacement energy of the InP (in a zincblende structure) is four times the dissociation energy of a In-P bond which is 2.05 eV [39].

	Ar^+ ions	**In**	**P**
Surface binding energy (eV)	0.0	2.49	3.27
Atomic volume (nm^3)	4.019×10^{-2}	2.607×10^{-2}	2.823×10^{-2}
Displacement energy (eV)	0.0	8.2	8.2

The Monte Carlo programme TRIDYN is essentially a ballistic simulation of ion/solid interactions. Therefore, the final depth distributions profiles were fitted to the ballistic model, equation (5). Figure 2 shows the averaged In profiles for different angles of ion incidence as calculated by TRIDYN. The *a* parameters obtained from the fit are given in Table 1. A plot of the calculated projected ranges, R_P and the fitted *a* parameters shows a definite cosine dependence on the angle of ion incidence, as shown in Figure 3. As can be seen from Figure 3, for small angles of incidence, the values are about equal but they deviate significantly at glancing angles; probably due to the effect of the surface vacancies.

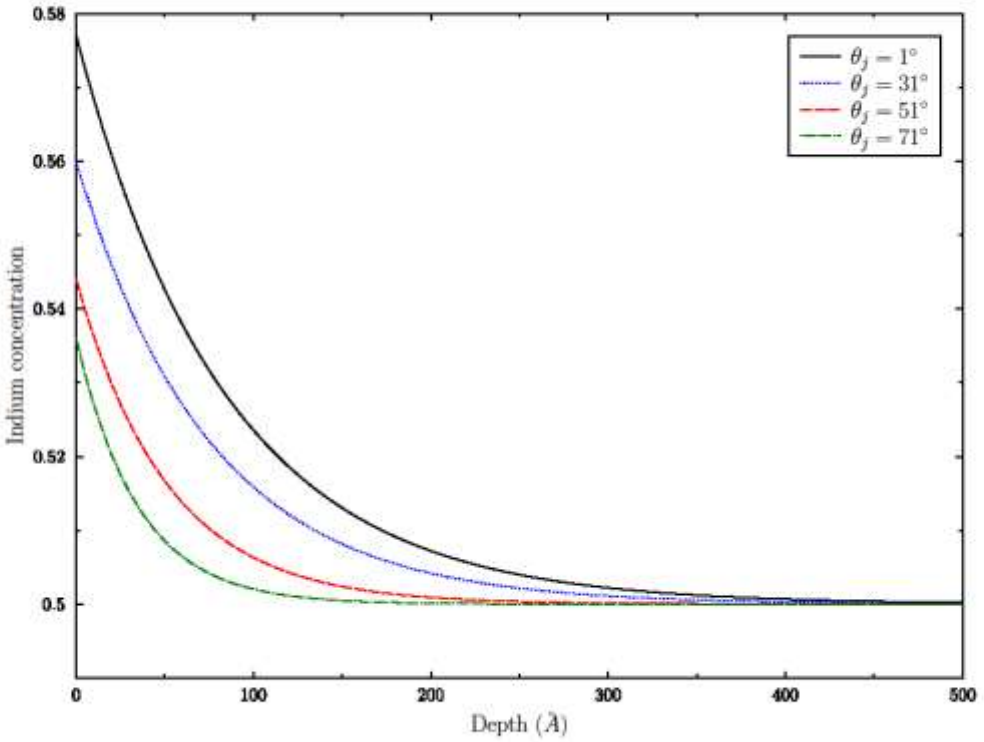

Figure 2. Indium concentration depth profiles for different angle of ion incidence, as calculated using TRIDYN.

As already mentioned, the ballistic model predicts disturbed layer thicknesses of around 6*a*. From Figure 2 it can be seen that for θ_j = 1° the altered layer is of the order of 48 nm. As preferential sputtering [40] takes place in the outer surface layer, i.e. the top 1-2 atomic layers, mixing of the target atoms via recoil implantation is responsible for a far thicker altered layer. Obviously, as can be seen from Figure 2, at higher ion incidence angles, the mixed layer becomes smaller as expected due to the shallower penetration of the ion into the target.

5. Discussion of the deconvoluted results

As was already indicated in section 4.2 no results with a surface concentration C_i^s between 0 and 1, could be obtained using the segregation dominated depth distribution function. Thus, the deconvoluted results presented here were calculated using only the ballistic model.

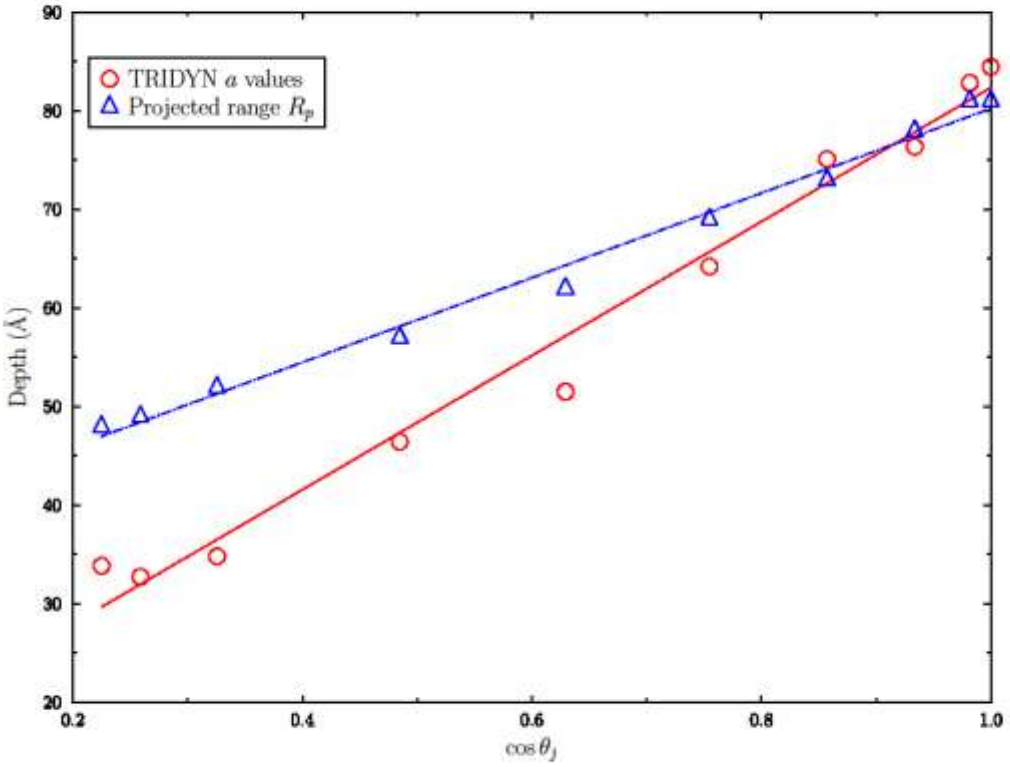

Figure 3. Calculated projected ranges, R_P for 5 keV Ar^+ ions in InP as well as the altered layer thickness parameter a fitted from TRIDYN profiles shown in Figure 2. A strong cosine dependence exists as a function of the ion angle of incidence.

The ballistic distribution function, equation (5), was substituted in equation (2), and rearranged to calculate the top-most surface concentration C_i^s, by substituting the measured Auger intensity ratio I_{In} / I_P and the standard intensities (as described in the experimental section) I_{In}^0 / I_P^0.

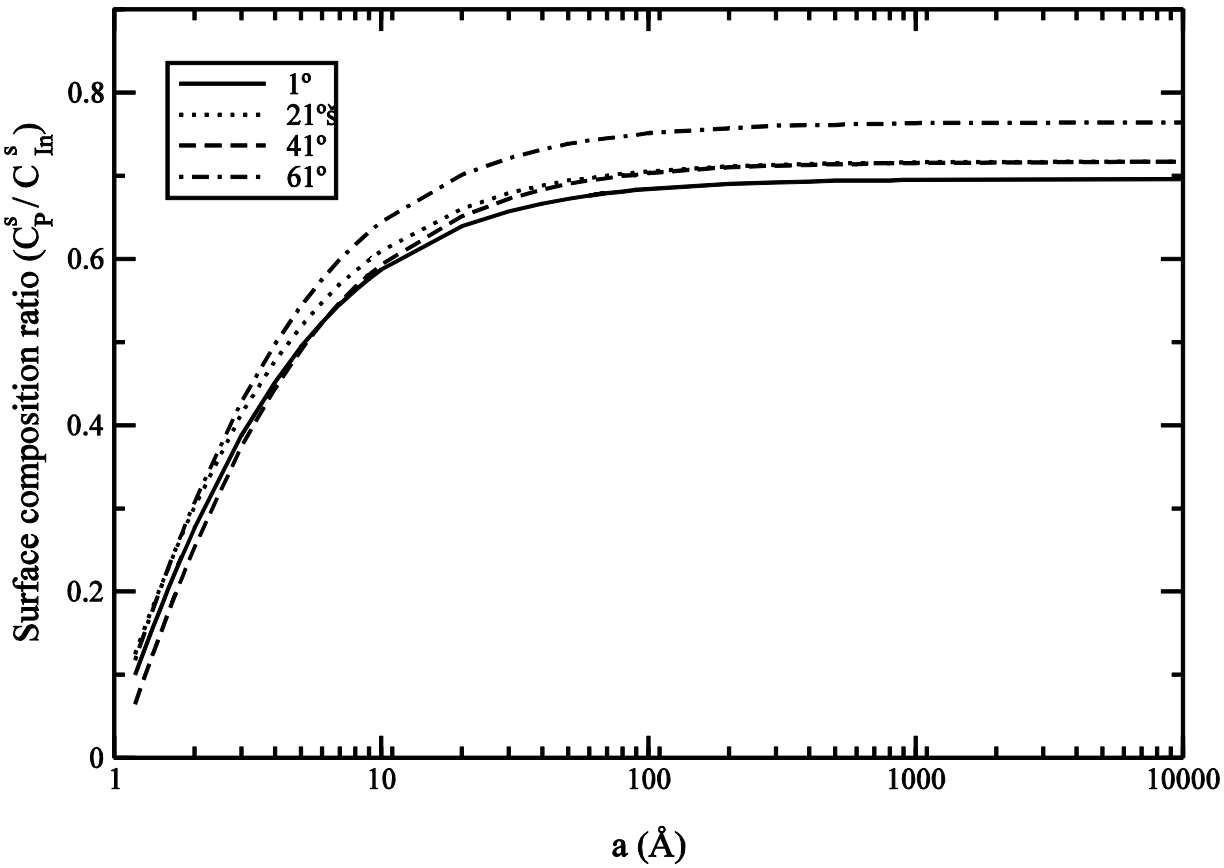

Figure 4. Surface composition ratios, C_P^s / C_{In}^s, after argon ion bombardment of an InP(100) surface. The variation of the surface compositions as a function of the disturbed layer thickness a are given for four different values of the ion angle of incidence θ_j. It can clearly be seen that there is a limit value a_l for which there is no change in the surface composition.

The a parameters estimated from the TRIDYN profile fits were used in equation (5) to describe the In and P depth distributions. Figure 4 shows the dependence of the deconvoluted surface compositions on the altered layer thickness parameter a for different angles of ion incidence. It can also be clearly seen that there is a definite limit value, a_l; for values larger than a_l, the resulting surface composition remains unchanged. Since this limit is well below the total disturbed layer thickness, it implies that atomic mixing is of secondary importance in influencing the surface composition, and confirms that preferential sputtering dominates. Furthermore, this indicates that the surface compositions obtained from the ballistic profile are not sensitive to the altered layer thicknesses, but to the exponential behaviour in the near surface region of the depth distribution function. Thus, using the projected ranges, R_P, instead of the fitted a parameters, give essentially the same result. This implies that quick SRIM calculations for R_P can be used to give an estimate of the altered layer parameter a; this will, however, not give a true reflection of the disturbed layer thickness.

The deconvoluted surface composition ratios C_P^s/C_{In}^s are shown in Figure 4 as a function of the cosine of the ion angle of incidence θ_j. Also shown are the surface composition ratios obtained from the TRIDYN simulations. The calculated

agreement between the measured and simulated surface composition ratios is good, viz. less than 5% except for the θ_j = 31° data point, for which the difference is 7.6%.

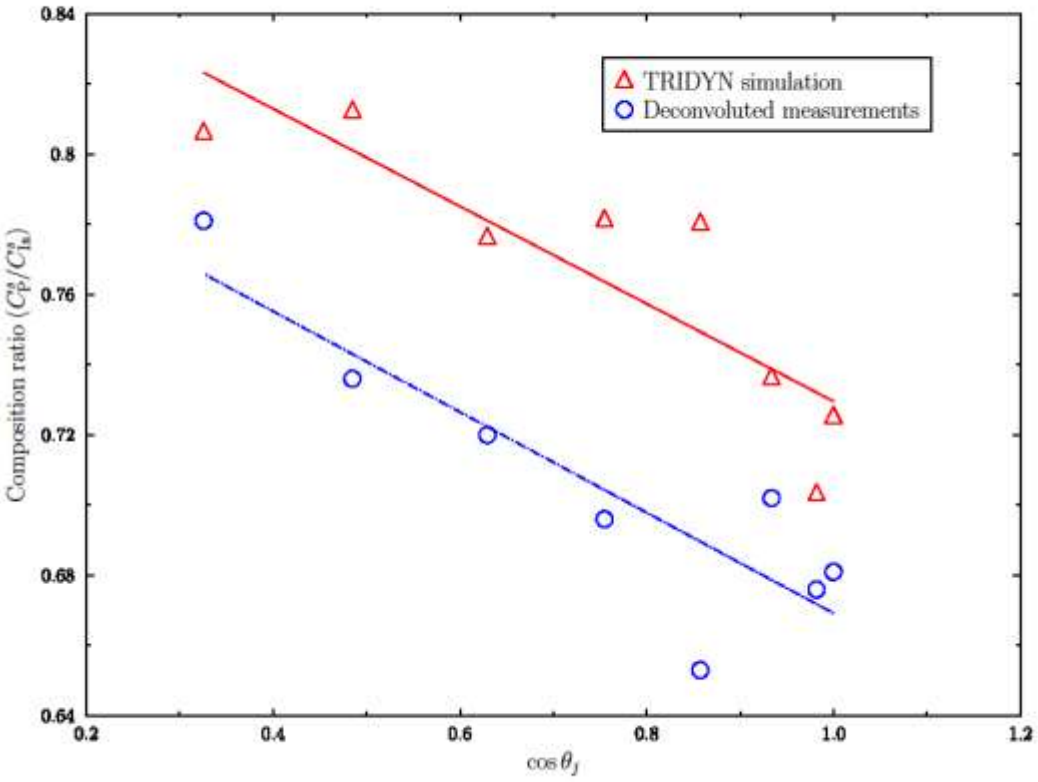

Figure 5. Surface composition ratios, C_P^s / C_{In}^s, as calculated from TRIDYN, as well as measured experimentally, using the ballistic deconvolution model described in section 4.3. The surface composition ratios is shown as a function of the ion angle of incidence θ_j, and shows strong $(\cos\theta_j)^f$ dependence, in line with the predictions from the model proposed by Malherbe [7]. The straight lines are least-squares linear fits to the data with slopes of -0.143 for the TRIDYN simulation values and -0.139 for the measured values.

The surface composition ratio shows a strong cosine dependence on the ion angle of incidence. This dependence on the ion angle of incidence has previously been discussed by Malherbe [7, 18, 41], and showed that the exponent f in $(\cos\theta_j)^f$ is a material dependent parameter. The surface composition ratios show a preferential removal of P from the target in agreement with most other authors (see Figure 6. This enrichment of In becomes less for more grazing angles of incidence. This corresponds with the effective altered layer depth; that is, there are fewer target atoms being mixed, and therefore less P atoms being transported to the surface. The fact that the experimental and TRIDYN values have the same trend with respect to $\cos\theta_j$ again indicates that ballistic (i.e. preferential sputtering with atomic mixing) effects

are the dominant mechanisms causing the deviation of the surface composition from stoichiometry. The difference in the actual values of the experimental and TRIDYN results is, thus, either due to systematic errors in the Auger measurements or due to long range radiation-induced diffusional effects.

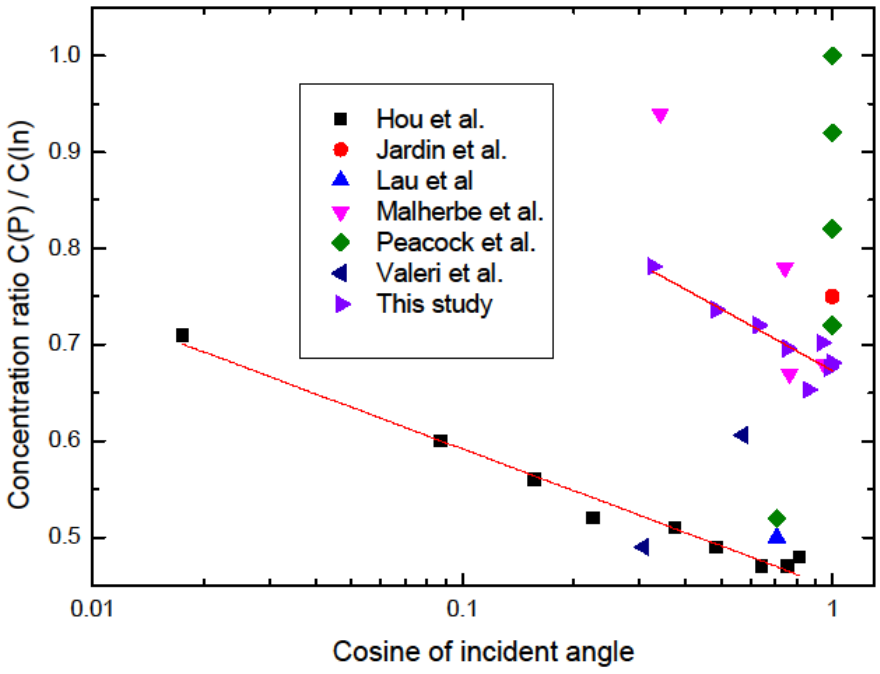

Figure 6. Averaged surface composition ratios, C_P^s/C_{In}^s, as determined with AES, XPS, SIMS, and ELS by various authors after Ar^+ ion bombardment [12, 18, 42-45].

There are two main sources for possible systematic errors in the measurements. The one is the assumption that the cleaved InP(110) surface has the same matrix as that of the sputtered surfaces. It is known [46] that crystallinity can affect the In to P Auger peak ratios. In our experiment, InP samples with two different crystal orientations were used to determine this effect. Both these samples gave the same In to P ratio, suggesting that we can ignore crystallinity effects in the determination of the standard. Furthermore, the InP(110) surface is a stiochiometric one. InP is a covalent bonded semiconductor which is readily amorphised by ion bombardment [7, 47]. Therefore, it is highly unlikely that crystal orientation effects will play any role in the Auger measurements on the sputtered surfaces. Previous studies [18, 41] also found no evidence of crystal orientation effects.

Bombardment-induced topography may also influence the average surface composition as measured by AES. It is well known that severe topography develops on InP with noble gas ion bombardment. It has been shown that the extent and form of topography depend on both the ion fluence [27] and the angle of incidence of the ions [28]. The AES surface compositions measured in this study and in others [18, 41]

remained constant for a particular ion energy and angle of incidence from a low fluence of 1×10^{15} Ar^{+} cm^{-2} to much higher doses (even as high as 5×10^{17} Ar^{+} cm^{-2}. An AFM study [27] showed that at a fluence of 1×10^{15} Ar^{+} cm^{-2}, the rms roughness of the surface were about the same as that of a virgin sample. The AFM images of the surface also showed that very little topography developed at this low dose. As also reflected in AFM images, the rms roughness increased with increasing dose. However, as was mentioned above, the measured surface concentrations remained constant with dose. Thus, it must be concluded that the bombardment-induced topography did not influence the results presented here. An ISS investigation [17] also found that the ISS spectra remained almost constant with increasing dose while the surface became covered with cones.

As was mentioned, apart from systematic errors, the other source for the discrepancy between the two sets of values in Figure 5 is long range diffusion. Figure 6 gives a selection of reported enrichment factors of In for InP under argon ion bombardment. The major differences in the measured values are probably due to the different experimental arrangements and conditions used. Direct AES measurements average the composition over the escape depth of the Auger electrons, while the method presented here calculates the top-most surface composition. In different AES systems, the sample surface orientations with respect to the incident electron beam and with respect to the analysers are different from each other. As is clear from the present paper, these will change the analysis volume, and thereby, the average ``surface'' composition.

Apart from the differences in analysis depth due to either different ion angles of incidence, or the different experimental setups, different ion bombardment conditions may also explain the differences between the reported results. These may include the ion energy and the fluence rate. These parameters may influence the diffusion in the altered layer. There has been no systematic study investigating the influence of the fluence rate on the equilibrium surface composition of InP. However, there have been several studies investigating the effect of ion energy. Several studies found no effect of argon ion energy on the equilibrium surface compositions [14, 18, 25, 42, 48-50]. This is in agreement with the well-known models of preferential sputtering [24, 40, 51-53]. Only near the threshold energy for sputtering do sample energy transfer considerations show that preferential sputtering effects should be ion energy dependent [54]. For all the above reported studies, the ion energies were all above this threshold energy [2]. Nevertheless, there are also a few studies [12, 15, 44, 55] that did report an energy dependence. Two groups [12, 15, 55] reported that with increasing ion energy, the surface composition becomes increasingly indium enriched, while the other group [44] obtained a contrary result.

From the above discussion it is clear that the influence of ion energy on the final surface composition has not been conclusively settled. This might be linked to the influence of the fluence rate which can also influence radiation-induced diffusion in

the altered layer.

The agreement between the TRIDYN simulations and the measured surface compositions is good. Least-squares fits of the cosine of the ion angle of incidence and the surface composition ratios obtained from the experiment and the TRIDYN simulations give slopes that are very similar; $f = 0.139$ for the experimental values, and $f = 0.143$ for the TRIDYN simulations (see Figure 5). The TRIDYN simulations showed that the effective altered layer is much larger than the projected range of the bombarding argon ions in agreement with other studies [50, 56]. However, the ballistic model described is an exponential type distribution in which the major redistribution of surface atoms takes place in a region of thickness $a \approx 1 - 2$ monolayers; essentially preferential sputtering. Mixing of target atoms take place in a region up to a depth estimated as $6a$. This mixing is probably due to recoil implantation of near-surface target atoms. No segregation behaviour can be deduced from the resulting TRIDYN profiles obtained. As already mentioned, no implantation of argon ions was considered in the simulations; it is assumed that minimal argon incorporation in the target matrix will occur, and thus have no effect on the sputtering yields. The effect of argon implantation on the resulting sputtering yield is still needs to be investigated.

The observed enrichment of In in the surface layer is thus mainly due to preferential sputtering of P, and to a lesser degree to atomic mixing, i.e. recoil implantation and diffusion migration with a strong possibility of radiation-induced diffusion also playing a part. According to the Sigmund theory [24, 40] the preferential sputtering in InP is mainly due to the large difference in the atomic masses of the two components. Furthermore, the surface binding energy (SBE) of In is larger than that for P, thereby enhancing the preferential removal of phosphorous. Malherbe [7] has argued that some spike sputtering is also possible in InP for low-energy Ar^+ bombardment, and that there is a greater probability for a spike volume to reach the surface at glancing angles. In such a spike volume both components will have similar kinetic energies, and thus the mass and SBE differences are not important. This gives a further argument for the cosine dependence of the enrichment of In.

6. Conclusions

It has been shown that simple atomic depth distribution functions can be used to deconvolute the instantaneous surface compositions in contrast to the usual averaged surface composition over many surface atomic layers, from measured Auger intensities taken at different angles. The depth distributions used, was based on either ballistic, chemical or both these considerations. This deconvolution method has been applied to the case of argon bombarded InP.

A segregation dominated depth distribution did not give results for which the fitted

mole fraction surface concentrations C_i^s were between 0 and 1. In contrast, the ballistic model can be fitted using easily determined parameters like the projected range of Ar^+ in InP. The resulting measured surface composition ratios C_P^s / C_{In}^s agreed very well with that determined from TRIDYN simulations.

The results confirmed that preferential sputtering is the dominant mechanism leading to non-stoichiometric surface compositions, i.e. an enrichment of indium was found in the altered layer. Atomic mixing and knock-on effects led to an altered layer of thickness of approximately 6*a*, where *a* is the fitting parameter used in the depth distribution function given by equation (5). Furthermore, there exist a very strong dependence of the steady-state surface composition on the ion angle of incidence, but no crystal orientation dependence could be found.

7. References

1. L. Ruben, J. Poate, Ion implantation in silicon technology, The Industrial Physicist 9 (2003) 12-15.
2. J.B. Malherbe, Sputtering of compound semiconductor surfaces. I. Ion-solid inter-actions and sputtering yields, CRC Crit. Rev. Solid State Mater. Sci. **19** (1994) 55 -127.
3. M. P. Seah, in Practical Surface Analysis: Volume 1 – Auger and X -ray Photoelectron Spectroscopy , 2nd Edn, ed. by D. Briggs and M. P. Seah, Chapt. 5. Wiley, Chichester (1990).
4. J.B. Malherbe, R Q Odendaal, Models for the sputter correction factor in quantitative AES of compound semiconductors, Surf. Interface Anal. 26 (1998) 841 – 850.
5. W. Liang, X. Wang, J. Guo, X. Wang, Preferential sputtering on multicomponent optical surfaces, Nucl. Intrum. Methods Phys. Res. B 410 (2017) 153-157.
6. H.M. Urbassek, M.L. Nietiadi, R.M. Bradley, G. Hobler, Sputtering of Si_cGe_{1-c} nanospheres, Phys. Rev. B 97 (2018) 155408.
7. J.B. Malherbe, Sputtering of compound semiconductor surfaces. II Compositional changes, radiation-induced topography and damage, CRC Crit. Rev. Solid State Mater. Sci. 19 (1994) 128 -195.
8. S. Hofmann, Y.S. Han, J.Y. Wang, Depth resolution and preferential sputtering in depth profiling of sharp interfaces, Appl. Surf. Sci. 410 (2017) 354-362.
9. R. Simpson, R.G. White, J.F. Watts, M.A. Barker, XPS investigation of monoatomic and cluster argon ion sputtering of tantalum pentoxide, Appl. Surf. Sci. 405 (2017) 79-87
10. E. Despiau-Pujo, P. Chabert, D.B. Graves, Molecular dynamics simulation of GaAs sputtering under low-energy argon ion bombardment, J. Vac. Sci. Technol. A 26 (2008) 274-280.
11. T. D. Bussing, P. H. Holloway, Y. X. Wang, J. F. Moulder, and J. S. Hammond, Composition depth profiles of oxidized silicon and sputtered GaAs

from angle resolved x-ray photoelectron spectroscopy, J. Vac. Sci. Technol. B 6 (1988) 1514-1518.
12. S. Valeri, M. Lolli, AES, EELS and XPS study ion-induced GaAs and InP (110) surface and subsurface modifications, Surf. Interface Anal. 16 (1990) 59-64.
13. I.L. Singer, J.S. Murday, R.L. Cooper, Surface composition changes in GaAs due to low-energy ion bombardment, Surf. Sci. 108 (1981) 7-24.
14. J B Malherbe, W O Barnard, Preferential sputtering of InP: An AES investigation, Surf. Sci. 255 (1991) 309 – 320.
15. S. Valeri, M. Lolli, P. Sberveglieri, AES and EELS study of alkali-metal absorption kinetics on either cleaved or sputtered GaAs and InP (110) surfaces, Surf. Sci. 238 (1990) 63-74.
16. M. Kalitzova, D. Karpuzov, Ts. Marinova, V. Krastev, G. Vitali, C. Pizzuto, G. Zollo, InP crystals-ion implantation and laser annealing: RHEED, XPS and computer simulation studies, Appl. Surf. Sci. 115 (1997) 1-9.
17. H.-I. Lee, T. Akita, R. Shimizu, Surface characterization for sputtter-cone formation on InP(100), Surf. Sci. 412-413 (1998) 24-29.
18. J B Malherbe, Ion angle dependence in the preferential sputtering of InP, Appl. Surf. Sci. 70/71 (1993) 322 – 326.
19. J.S. Pan A.T.S. Wee, C.H.A. Huan, H.S. Tan, K.L. Tan, Argon incorporation and surface compositional changes in InP(100) due to low-energy Ar^+ ion bombardment, J. Appl. Phys. 80 (1996) 6655-6660.
20. W. Yu, J.L. Sullivan, S.O. Saied, G.A.C. Jones, Ion bombardment induced compositional changes in GaP and InP surfaces, Nucl. Instrum. Methods Phys. Res. B 135 (1998) 250-255.
21. M. Tanemura, T. Aoyama, A. Otani, M. Ukita, F. Okuyama, C.K. Chini, Angular distributions of In and P particles sputtered from InP by inert-gas ion bombardment, Surf. Sci. 376 (1997) 163-168.
22. J. Zemek, O.A. Baschenko, M.A. Tyzykhov, P. Jiricek, Altered layer composition of sputtered InP(100) wafers: non-destructive concentration depth profiling, Surf. Sci. 318 (1994) 421-427.
23. V.S. Chernysh, H.H. Brongersma, P. Brüner, T. Grehl, Surface composition of ion bombarded nickel based alloys, Nucl. Instrum. Methods Phys. Res. B 52 (2019) in press.
24. P. Sigmund, A. Oliva, Alloy sputtering at high fluence: preferential sputtering and competing effects, Nucl. Instrum. Methods Phys. Res. B 82 (1993) 269 – 282.
25. J.B. Malherbe, N.G. van der Berg, Argon bombardment-induced topography development on InP, Surf. Interface Anal. 22 (1994) 538-542.
26. A. Savitzky, M.J.E. Golay, Smoothing and differentiation of data by simplified least squares procedures, Anal. Chem. 36 (1964) 1627-1639.
27. C.M. Demanet, J.B. Malherbe, N.G. van der Berg, V. Sankar, Atomic force microscopy investigation of argon-bombarded InP: Effect of ion dose density, Surf. Interface Anal. **23** (1995) 433-439.
28. C.M. Demanet, K. Vijaya. Sankar, J.B. Malherbe, Atomic force microscopy

investigation of ion-bombarded InP: Effect of angle of ion bombardment, Surf. Interface Anal. 24 (1996) 503-510.
29. C.M. Demanet, K. Vijaya. Sankar, J.B. Malherbe, N.G. van der Berg, R.Q. Odendaal, Atomic force microscopy investigation of noble gas ion-bombardment on InP: Effect of ion energy, Surf. Interface Anal. 24 (1996) 497-502.
30. A. Jablonski, S. Tougaard, Escape probability of electrons from solids, Surf. Sci. 432 (1999) 211-227.
31. S. Hofmann, Practical Surface Analysis by Auger and X-ray Photoelectron Spectroscopy (Wiley, Chichester, 1990) Chap. 4.
32. R. Shimizu, Quantitative analysis by Auger electron spectroscopy, Jpn. J. Appl. Phys. 22 (1983) 1631-1642.
33. Y. Shimotsuma, S Ichimura, Backscattering correction for AES spectra measured at oblique angles (> 45°) incidence of primary electron beam, Surf. Interface Anal. 31 (2001) 102-105.
34. S. Tanuma, C.J. Powell, D.R. Penn, Calculation of electron inelastic mean free paths. III Data for 15 inorganic compounds over the 50-2000 eV range, Surf. Interface Anal. 17 (1991) 927-939.
35. W. Moller, W. Eckstein, J.P. Biersack, TRIDYN - binary collision simulation of atomic collisions and dynamic composition changes in solids, Comp. Phys. Comm. 51 (1988) 355-368.
36. http://www.srim.org., Accessed on 13 February 2018.
37. G. Ecke, R. Kosiba, V. Kharlamov, Y. Trushin, J. Pezoldt, The estimation of sputtering yields for SiC and Si, Nucl. Intrum. Methods Phys. Res. B 196 (2002) 39-50.
38. J.A. Kerr, in: CRC Handbook of Chemistry and Physics, Ed. R.C. West, 69th ed. (CRC Press, Cleveland, OH, 1988) pp. Fl74-F182.
39. J.A. Kerr, in: CRC Handbook of Chemistry and Physics, Ed. R.C. West, 73rd ed. (CRC Press, Cleveland, OH, 1992) pp. 9-129.
40. P. Sigmund, Sputtering by Particle Bombardment I, (Springer, Berlin, 1981) Chap. 2.
41. J.B. Malherbe, N.G. van der Berg, Surface compositional changes of InP due to krypton ion bombardment Surf Interface Anal 22 (1994) 543-546.
42. W.N. Lau, R.N.S. Sodhi, B.J. Flinn, K.H. Tan, G.M. Bancroft, Photoemission study of sputter-etched InP surfaces, Appl. Phys. Lett. 51 (1987) 177-179.
43. X. Hou, M. Yu, X Wang, The variation of In islands on InP surface, Chin. Phys. Lett. 2 (1985) 31-34.
44. D.C. Peacock, An AES, SAM and RHEED study of InP subjected to ion bombardment and annealing treatments, Vacuum 33 (1983) 601-605.
45. C. Jardin, D. Robert, B. Achard, B. Gruzza, C. Pariset, An AES and ELS study of InP(100) surface subjected to argon ion bombardment, Surf. Interface Anal. 10 (1987) 301-305.
46. S. Valeri, A. di Bona, E. Nava, Diffraction effects in Auger quantitative analysis on III-V compounds, Appl. Surf. Sci. 70-71 (1993) 20-23.

47. E. Friedland, Radiation damage in metals, CRC Crit. Rev. Solid State Mater. Sci. 25 (2001) 87-143.
48. X. Hou, M. Yu, X Wang, Experimental evidence for indium island formation on clean InAs and InSb surfaces, Chin. Phys. 7 (1987) 854-856.
49. A. Barcz M. Croset, L.M. Mercandalli, Quantitativity in III-V compouinds by low-energy ion scattering spectrometry (ISS), Surf. Sci. 95 (1980) 511-526.
50. R.S. Williams, Low energy Ar ion bombardment damage of Si, GaAs and InP surfaces Solid State Comm. 41 (1982) 153-156.
51. R. Kelly, Chemistry and Physics of Solid Surfaces V (Springer, Berlin, 1984) Chap 7.
52. H.H. Anderson, Ion Implantation and Beam Processing (Academic Press, Sydney, 1984) Chap. 6.
53. J B Malherbe, S Hofmann & J M Sanz, Preferential sputtering of oxides: A comparison of model predictions with experimental data, Appl. Surf. Sci. 27 (1986) 355-365.
54. E. Taglauer, Probing surfaces with ions, Surf. Sci. 299-300 (1994) 64-76.
55. J. Morais, T.A. Fazan, R. Landers, Ion induced composition changes on (110) InP cleaved surfaces, Phys. Status Solidi (a) 141 (1994) K19-K21.
56. S. Valeri, G.C Gazzadi, A. Rota, A. di Bona, Early stages of low energy ion-induced damage in InP, Appl. Surf. Sci. 120 (1997) 323-334.